MechCADemy Notes: Theory Meets Practice

From Potential Energy to Finite Elements

Minimum Potential Energy and the Rayleigh–Ritz Method

A Physics-First Route to $\boldsymbol{Ka} = \boldsymbol{F}$

Dr. Iman Salehinia

Associate Professor of Mechanical Engineering

Northern Illinois University, DeKalb, USA

September 2026

Your support matters! Please subscribe to the MechCADemy YouTube channel, share the videos and notes with others, and send comments and suggestions to help improve future educational content.

Download this Academy Note

The current Academy Notes and supporting educational material can be downloaded from the MechCADemy webpage.

Purpose of these notes

These notes connect potential energy, stable equilibrium, the Rayleigh–Ritz method, and the finite element method. The development is intentionally deeper than a lecture script: definitions are separated carefully, derivations are shown step by step, and examples expose both the power and the limitations of displacement-based approximations.

Contents

1 Why Potential Energy Matters in Structural Analysis **3**
1.1 Strain energy and external work: start with a spring . . . 3
1.2 The principle of minimum potential energy . . . 4

2 Potential Energy of Discrete and Continuous Structures **4**
2.1 A three-spring assembly . . . 4
2.2 An axial bar: from coordinates to a displacement function . . . 5
2.3 General elastic continuum . . . 6
2.4 Euler–Bernoulli beam . . . 7

3 The Rayleigh–Ritz Method: A Finite Search **8**
3.1 The method, step by step . . . 8
3.2 Worked global example: an axially loaded bar . . . 9
3.3 Cantilever beam: one term and two terms . . . 10
3.4 Worked example: a two-dimensional two-bar truss . . . 11
3.5 Worked example: a simply supported beam under a center load . . . 12

4 From Global Rayleigh–Ritz to the Finite Element Method **13**

4.1 Trial functions, coefficients, and nodal degrees of freedom . . . 13
4.2 From displacement interpolation to the algebraic equilibrium equations . . . 14
4.3 Worked specialization: an Euler–Bernoulli beam element . . . 16
4.4 A two-node axial bar element . . . 17
4.5 Finite-element example: the same linearly loaded bar . . . 18
4.6 Extension beyond structures: acoustic modes of a rigid cavity . . . 19

5 Thermal Strains, Initial Strains, and Residual Stresses 20

6 Deeper Understanding After the Method Is Clear 21
6.1 Why the continuum problem becomes finite . . . 21
6.2 Finite coefficient equations versus pointwise equilibrium . . . 21
6.3 Why displacement usually converges faster than stress . . . 21
6.4 Artificial stiffness: physical meaning, consequences, and remedies . . . 22

7 Connection to Weighted-Residual and Galerkin Methods 23

8 Problem for Further Study 24

9 Compact Formula Summary 24

10 Concluding Perspective 25

References 26

CAD FEA Design
MechCADemy

1 Why Potential Energy Matters in Structural Analysis

Finite element analysis is often summarized by

$$\boldsymbol{K}\boldsymbol{a} = \boldsymbol{F}. \tag{1.1}$$

The equation is compact, but it does not by itself explain where stiffness comes from, why displacement functions matter, or why FEA is approximate. A useful route to those answers begins with energy. For a conservative elastic structure,

$$\Pi = U_{\mathrm{el}} - W_{\mathrm{ext}}, \tag{1.2}$$

where Π is the **potential energy** of the structure, U_{el} is the total elastic strain energy stored by deformation, and W_{ext} is the work done by the applied loads.

1.1 Strain energy and external work: start with a spring

For a linear spring of stiffness k, force increases from zero to ku as the spring extends. The stored energy is the area under the force–displacement curve:

$$U_{\mathrm{el}} = \int_0^u k\hat{u}\ \mathrm{d}\hat{u} = \frac{1}{2}ku^2. \tag{1.3}$$

A constant external force P acting through u performs work $W_{\mathrm{ext}} = Pu$, so

$$\Pi(u) = \frac{1}{2}ku^2 - Pu. \tag{1.4}$$

The continuum analogue begins with *elastic strain-energy density*, which is the elastic energy stored per unit volume. Under uniaxial loading, its increment and accumulated value are

$$\mathrm{d}U_e = \sigma\ \mathrm{d}\varepsilon, \qquad U_e(\varepsilon) = \int_0^\varepsilon \sigma(\tilde{\varepsilon})\ \mathrm{d}\tilde{\varepsilon}. \tag{1.5}$$

Geometrically, U_e is the area under the stress–strain curve. For linear elasticity, $\sigma = E\varepsilon$, and therefore

$$U_e = \int_0^\varepsilon E\tilde{\varepsilon}\ \mathrm{d}\tilde{\varepsilon} = \frac{1}{2}E\varepsilon^2 = \frac{1}{2}\sigma\varepsilon. \tag{1.6}$$

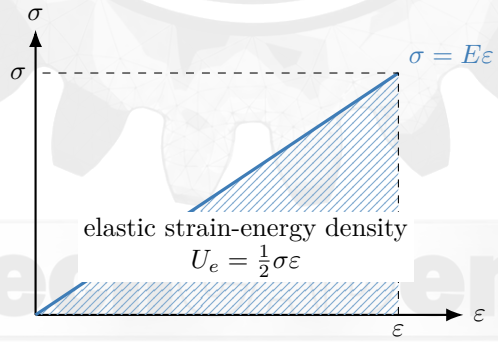


Figure 1: For linear elasticity, elastic strain-energy density is the triangular area under the stress–strain curve.

The total elastic strain energy is obtained by accumulating this energy density throughout the body:

$$U_{\mathrm{el}} = \int_V U_e\ \mathrm{d}V = \int_V \left(\int_0^\varepsilon \sigma(\tilde{\varepsilon})\ \mathrm{d}\tilde{\varepsilon} \right) \mathrm{d}V. \tag{1.7}$$

Thus $\int \sigma\ \mathrm{d}\varepsilon$ is an energy density, $\int_V U_e\ \mathrm{d}V$ is the total elastic strain energy, and $\frac{1}{2}\sigma\varepsilon$ is the special linear-elastic energy density for loading from an unstressed reference state. For nonlinear elasticity the integral must generally be retained.

This definition also makes the amplitude scaling transparent. If a deformation pattern is multiplied by A, then strain and stress are each proportional to A in linear elasticity. Hence

$$U_e \propto \sigma\varepsilon \propto A^2, \qquad U_{\text{el}} \propto A^2, \qquad W_{\text{ext}} \propto A. \tag{1.8}$$

The quadratic stored energy and linear load work allow total potential energy to develop a minimum.

1.2 The principle of minimum potential energy

Potential energy measures the energy available because of configuration. In mechanics it is important because it combines internal deformation and external loading into one scalar quantity. If a conservative structure is displaced slightly from a stable equilibrium configuration, its total potential energy increases; the system therefore tends to return toward the lower-energy configuration. A stationary configuration may represent a minimum, maximum, or saddle point, but stable equilibrium is associated with a local minimum.

This provides a second route to equilibrium. Instead of balancing forces point by point at the outset, we compare kinematically allowable configurations and identify the stable one through energy.

Principle of minimum potential energy

Of all admissible displacement configurations that satisfy the prescribed displacement constraints, the stable equilibrium configuration locally minimizes

$$\Pi = U_{\text{el}} - W_{\text{ext}}.$$

For the one-degree-of-freedom spring,

$$\frac{\mathrm{d}\Pi}{\mathrm{d}u} = ku - P = 0 \qquad \Longrightarrow \qquad ku = P. \tag{1.9}$$

The energy calculation recovers equilibrium. For a continuum, however, the unknown is an entire displacement function. The Rayleigh–Ritz method converts that infinite-dimensional search into a finite one.

2 Potential Energy of Discrete and Continuous Structures

2.1 A three-spring assembly

Consider four nodes connected by three springs. Temporarily retain all four nodal displacements so that the complete matrix is visible.

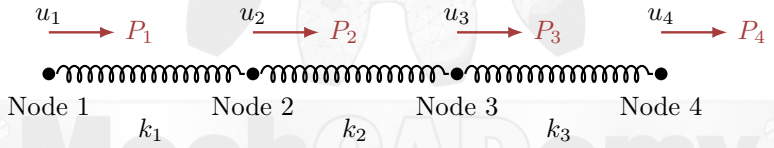


Figure 2: Three-spring assembly with four nodal displacement degrees of freedom.

The spring extensions are $u_2 - u_1$, $u_3 - u_2$, and $u_4 - u_3$, so

$$U_{\text{el}} = \tfrac{1}{2}k_1(u_2 - u_1)^2 + \tfrac{1}{2}k_2(u_3 - u_2)^2 + \tfrac{1}{2}k_3(u_4 - u_3)^2, \tag{2.1}$$

$$W_{\text{ext}} = P_1u_1 + P_2u_2 + P_3u_3 + P_4u_4. \tag{2.2}$$

The total potential energy is therefore

$$\Pi(\boldsymbol{u}) = \tfrac{1}{2}k_1(u_2 - u_1)^2 + \tfrac{1}{2}k_2(u_3 - u_2)^2 + \tfrac{1}{2}k_3(u_4 - u_3)^2 - \sum_{i=1}^{4} P_iu_i.$$

Because u_1, u_2, u_3, and u_4 are independent degrees of freedom, stationarity requires the derivative with respect to each displacement to vanish. Differentiating one degree of freedom at a time gives

$$\begin{aligned}
\frac{\partial \Pi}{\partial u_1} &= \tfrac{1}{2}k_1\,2(u_2-u_1)(-1) - P_1 = k_1(u_1-u_2) - P_1 = 0,\\
&\qquad\Longrightarrow\quad k_1u_1 - k_1u_2 = P_1,\\
\frac{\partial \Pi}{\partial u_2} &= \tfrac{1}{2}k_1\,2(u_2-u_1)(1) + \tfrac{1}{2}k_2\,2(u_3-u_2)(-1) - P_2\\
&= k_1(u_2-u_1) + k_2(u_2-u_3) - P_2 = 0,\\
&\qquad\Longrightarrow\quad -k_1u_1 + (k_1+k_2)u_2 - k_2u_3 = P_2,\\
\frac{\partial \Pi}{\partial u_3} &= \tfrac{1}{2}k_2\,2(u_3-u_2)(1) + \tfrac{1}{2}k_3\,2(u_4-u_3)(-1) - P_3\\
&= k_2(u_3-u_2) + k_3(u_3-u_4) - P_3 = 0,\\
&\qquad\Longrightarrow\quad -k_2u_2 + (k_2+k_3)u_3 - k_3u_4 = P_3,\\
\frac{\partial \Pi}{\partial u_4} &= \tfrac{1}{2}k_3\,2(u_4-u_3)(1) - P_4 = k_3(u_4-u_3) - P_4 = 0,\\
&\qquad\Longrightarrow\quad -k_3u_3 + k_3u_4 = P_4.
\end{aligned}$$

Collecting the coefficient of each nodal displacement in these four equations gives

$$\boxed{\begin{bmatrix} k_1 & -k_1 & 0 & 0\\ -k_1 & k_1+k_2 & -k_2 & 0\\ 0 & -k_2 & k_2+k_3 & -k_3\\ 0 & 0 & -k_3 & k_3 \end{bmatrix}\begin{bmatrix} u_1\\ u_2\\ u_3\\ u_4 \end{bmatrix} = \begin{bmatrix} P_1\\ P_2\\ P_3\\ P_4 \end{bmatrix}} \quad \text{or} \quad \boxed{\boldsymbol{K}\boldsymbol{u} = \boldsymbol{P}.} \tag{2.3}$$

The matrix is symmetric and every row sums to zero. Equal translation of all nodes stretches no spring, so the unrestrained matrix contains a rigid-body mode. After imposing $u_1 = 0$, rows 2–4 give the reduced 3×3 system, while the first row recovers the support reaction.

The direct stiffness method produces the same result. Each spring has

$$\boldsymbol{K}^{(e)} = k_e\begin{bmatrix} 1 & -1\\ -1 & 1 \end{bmatrix}. \tag{2.4}$$

Expanding each spring into the four-degree-of-freedom ordering gives

$$\begin{aligned}
\boldsymbol{K}_g^{(1)} &= \begin{bmatrix} k_1 & -k_1 & 0 & 0\\ -k_1 & k_1 & 0 & 0\\ 0 & 0 & 0 & 0\\ 0 & 0 & 0 & 0 \end{bmatrix}, \quad \boldsymbol{K}_g^{(2)} = \begin{bmatrix} 0 & 0 & 0 & 0\\ 0 & k_2 & -k_2 & 0\\ 0 & -k_2 & k_2 & 0\\ 0 & 0 & 0 & 0 \end{bmatrix},\\
\boldsymbol{K}_g^{(3)} &= \begin{bmatrix} 0 & 0 & 0 & 0\\ 0 & 0 & 0 & 0\\ 0 & 0 & k_3 & -k_3\\ 0 & 0 & -k_3 & k_3 \end{bmatrix}.
\end{aligned} \tag{2.5}$$

Their sum is exactly the energy-derived matrix. The two routes are different organizations of the same mechanics.

2.2 An axial bar: from coordinates to a displacement function

For a prismatic axial bar with length L, area A, modulus E, distributed load $q(x)$, and end load P,

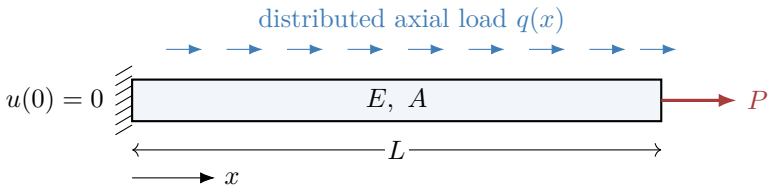


Figure 3: Axial bar with distributed axial load $q(x)$ and end force P.

$$\varepsilon = \frac{\mathrm{d}u}{\mathrm{d}x}, \qquad \sigma = E\varepsilon. \tag{2.6}$$

$$U_e = \int_0^{\varepsilon} E\tilde{\varepsilon}\ \mathrm{d}\tilde{\varepsilon} = \frac{1}{2}E\varepsilon^2 = \frac{1}{2}\sigma\varepsilon. \tag{2.7}$$

It is the triangular area in Fig. 1; it assumes linear elasticity, proportional loading from an unstressed state, and a linear stress–strain relation. Therefore

$$U_{\mathrm{el}} = \frac{1}{2}\int_0^L EA\left(\frac{\mathrm{d}u}{\mathrm{d}x}\right)^2 \mathrm{d}x, \tag{2.8}$$

$$W_{\mathrm{ext}} = \int_0^L q(x)u(x)\ \mathrm{d}x + Pu(L), \tag{2.9}$$

and

$$\boxed{\Pi[u] = \frac{1}{2}\int_0^L EA(u')^2\,\mathrm{d}x - \int_0^L q(x)u(x)\,\mathrm{d}x - Pu(L).} \tag{2.10}$$

The expression $\Pi[u]$ is a **functional**: the displacement field $u(x)$ is its input, and the corresponding potential energy is its scalar output. Functionals are central to the calculus of variations and to more advanced finite element derivations based on weak forms, so this terminology will be useful later.

Function, functional, and operator

A **function** maps numbers to numbers. A **functional** takes an entire function as input and assigns one scalar to it. Thus $\Pi[u]$ takes the complete admissible displacement field $u(x)$ and returns one number: its total potential energy. An **operator** generally maps a function to another function; for example, $\mathcal{L}[u] = u''$.
The total potential energy $\Pi[u]$ is a functional because it assigns a single value of total potential energy to each admissible displacement field $u(x)$.

2.3 General elastic continuum

For a three-dimensional state, the stress and strain components are arranged in vector form. This representation makes the constitutive and finite element equations easier to express and manipulate using matrix operations:

$$\boldsymbol{\sigma} = \begin{bmatrix}\sigma_{xx} & \sigma_{yy} & \sigma_{zz} & \tau_{xy} & \tau_{yz} & \tau_{xz}\end{bmatrix}^{\mathsf{T}}, \quad \boldsymbol{\varepsilon} = \begin{bmatrix}\varepsilon_{xx} & \varepsilon_{yy} & \varepsilon_{zz} & \gamma_{xy} & \gamma_{yz} & \gamma_{xz}\end{bmatrix}^{\mathsf{T}}. \tag{2.11}$$

The general incremental elastic strain-energy density is

$$\mathrm{d}U_e = \boldsymbol{\sigma} : \mathrm{d}\boldsymbol{\varepsilon}. \tag{2.12}$$

For linear elasticity,

$$\boldsymbol{\sigma} = \boldsymbol{D}\boldsymbol{\varepsilon}, \tag{2.13}$$

where $\boldsymbol{D}$ is the constitutive matrix that relates the stress and strain components. Introduce a proportional loading path

$$\boldsymbol{\varepsilon}(\lambda) = \lambda\boldsymbol{\varepsilon}, \qquad \boldsymbol{\sigma}(\lambda) = \lambda\boldsymbol{\sigma}, \qquad 0 \le \lambda \le 1. \tag{2.14}$$

Then

$$U_e = \int_0^1 \boldsymbol{\sigma}(\lambda) : \frac{\mathrm{d}\boldsymbol{\varepsilon}(\lambda)}{\mathrm{d}\lambda}\ \mathrm{d}\lambda \tag{2.15}$$

$$= \int_0^1 (\lambda\boldsymbol{\sigma}) : \boldsymbol{\varepsilon}\ \mathrm{d}\lambda = \frac{1}{2}\boldsymbol{\sigma} : \boldsymbol{\varepsilon}. \tag{2.16}$$

Thus

$$\boxed{U_e = \frac{1}{2}\boldsymbol{\sigma} : \boldsymbol{\varepsilon}}, \qquad \boxed{U_{\mathrm{el}} = \frac{1}{2}\int_V \boldsymbol{\sigma} : \boldsymbol{\varepsilon}\ \mathrm{d}V}. \tag{2.17}$$

With the engineering-strain vectors above, the double contraction is represented by

$$U_e = \frac{1}{2}\boldsymbol{\sigma}^{\mathsf{T}}\boldsymbol{\varepsilon}, \qquad U_{\mathrm{el}} = \frac{1}{2}\int_V \boldsymbol{\varepsilon}^{\mathsf{T}}\boldsymbol{D}\boldsymbol{\varepsilon}\ \mathrm{d}V. \tag{2.18}$$

Compatible stress/strain conventions are essential. If tensorial shear strains replace engineering shear strains, the vector expression requires the corresponding factors of two.

Body forces $\boldsymbol{b}$, surface tractions $\boldsymbol{t}$, and concentrated forces $\boldsymbol{P}_j$ give

$$\Pi[\boldsymbol{u}] = \frac{1}{2}\int_V \boldsymbol{\varepsilon}^{\mathsf{T}}\boldsymbol{D}\boldsymbol{\varepsilon}\,\mathrm{d}V - \int_V \boldsymbol{u}^{\mathsf{T}}\boldsymbol{b}\,\mathrm{d}V - \int_{S_t}\boldsymbol{u}^{\mathsf{T}}\boldsymbol{t}\,\mathrm{d}S - \sum_j \boldsymbol{u}_j^{\mathsf{T}}\boldsymbol{P}_j. \tag{2.19}$$

2.4 Euler–Bernoulli beam

The Euler–Bernoulli kinematic assumption is that a cross section initially plane and perpendicular to the neutral axis remains plane and perpendicular to the deformed neutral axis. The tangent to the deformed neutral axis gives

$$\tan\theta(x) = \frac{\mathrm{d}w}{\mathrm{d}x}. \tag{2.20}$$

For a small rotation, $\tan\theta \approx \theta$, and therefore

$$\boxed{\theta(x) \approx \frac{\mathrm{d}w}{\mathrm{d}x}}. \tag{2.21}$$

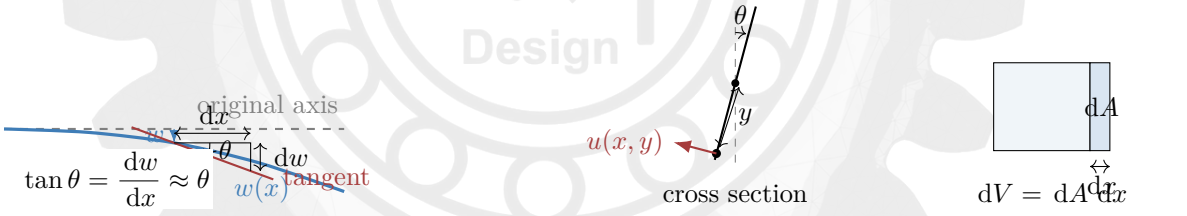
A material point a distance y from the neutral axis acquires axial displacement

$$\boxed{u(x,y) = -y\theta(x) = -y\frac{\mathrm{d}w}{\mathrm{d}x}}. \tag{2.22}$$

Therefore

$$\boxed{\varepsilon_x = \frac{\partial u}{\partial x} = -y\frac{\mathrm{d}^2 w}{\mathrm{d}x^2}}. \tag{2.23}$$

The sign depends on the selected axes and positive displacement convention; the important physical statement is that axial strain varies linearly through the depth and is proportional to curvature.



(a) Slope and rotation. (b) Axial displacement. (c) Differential beam slice.

Figure 4: Euler–Bernoulli displacement assumptions and the differential volume used in the energy integral.

For a beam slice, $\mathrm{d}V = \mathrm{d}A\,\mathrm{d}x$. This is not differentiation of the product Ax; it is an infinitesimal volume formed from cross-sectional area $\mathrm{d}A$ and axial length $\mathrm{d}x$. Consequently,

$$U_{\mathrm{el}} = \frac{1}{2}\int_V \sigma_x\varepsilon_x\,\mathrm{d}V = \frac{1}{2}\int_0^L\int_A \sigma_x\varepsilon_x\,\mathrm{d}A\,\mathrm{d}x, \tag{2.24}$$

$$\sigma_x\varepsilon_x = E\varepsilon_x^2 = Ey^2[w''(x)]^2. \tag{2.25}$$

Because E and $w''(x)$ are constant across a homogeneous cross section,

$$U_{\mathrm{el}} = \frac{1}{2}\int_0^L E[w''(x)]^2\left(\int_A y^2\,\mathrm{d}A\right)\mathrm{d}x \tag{2.26}$$

$$= \boxed{\frac{1}{2}\int_0^L EI[w''(x)]^2\,\mathrm{d}x}, \qquad I = \int_A y^2\,\mathrm{d}A. \tag{2.27}$$

For transverse load $q(x)$, point loads P_j, and point moments M_j,

$$\Pi[w] = \frac{1}{2}\int_0^L EI(w'')^2\,\mathrm{d}x - \int_0^L q(x)w(x)\,\mathrm{d}x - \sum_j P_j w(x_j) - \sum_j M_j w'(x_j). \tag{2.28}$$

A numerical method requires a finite-dimensional search space. The Rayleigh–Ritz method provides that step.

3 The Rayleigh–Ritz Method: A Finite Search

The preceding section established that equilibrium is found by making the potential energy stationary. For a continuum, however, the unknown is an entire displacement function rather than a finite list of numbers. Searching directly through every admissible function is not practical, so a systematic approximation method is needed.

The Rayleigh–Ritz method provides that bridge. It replaces the unlimited search over admissible displacement fields with a finite search over carefully selected displacement shapes [1, 3]. The reason for introducing the method is therefore direct: it gives us a practical way to approximate the displacement field that makes Π stationary.

3.1 The method, step by step

Approximate the unknown field by

$$u^h(x) = \sum_{i=1}^{n} A_i \phi_i(x). \tag{3.1}$$

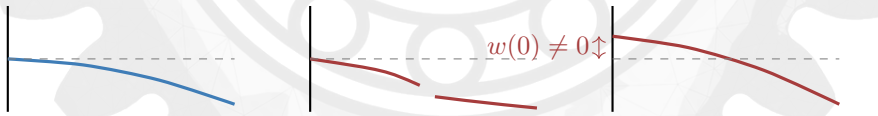
The functions ϕ_i are fixed in advance; the Ritz coefficients A_i determine how much of each shape appears in the approximation.



(a) One search direction. (b) Two search directions.

Figure 5: Rayleigh–Ritz trial families: adding independent admissible functions enriches the approximation space.

Every trial function must satisfy the prescribed displacement boundary conditions and must possess the continuity required by the energy expression. An axial bar fixed at $x = 0$ requires $\phi_i(0) = 0$. An Euler–Bernoulli cantilever requires both $\phi_i(0) = 0$ and $\phi_i'(0) = 0$ because its energy contains w''.



(a) admissible (b) gap / improper kink (c) nonzero shift at clamp

Figure 6: Trial-function examples for a clamped beam: (a) admissible, (b) inadmissible because of a gap or improper kink, and (c) inadmissible because the clamp displacement is violated.

After substitution, the functional becomes an ordinary multivariable function:

$$\Pi[u^h] \longrightarrow \Pi(A_1, A_2, \ldots, A_n). \tag{3.2}$$

Its total differential is

$$\boxed{\mathrm{d}\Pi = \sum_{i=1}^{n} \frac{\partial \Pi}{\partial A_i}\, \mathrm{d}A_i}. \tag{3.3}$$

At a stationary point, $\mathrm{d}\Pi = 0$. Because $\mathrm{d}A_1, \ldots, \mathrm{d}A_n$ are independent choices, the statement must remain true regardless of which coefficient is changed. Therefore the coefficient multiplying every independent $\mathrm{d}A_i$ must vanish:

$$\boxed{\frac{\partial \Pi}{\partial A_i} = 0, \qquad i = 1, 2, \ldots, n.} \tag{3.4}$$

These equations determine the unknown coefficients. For a linear elastic problem they form a linear algebraic system.

The Rayleigh–Ritz method in one sentence

Choose a finite set of admissible displacement shapes, scale and superpose them with unknown Ritz coefficients, insert the approximation into total potential energy, and determine the coefficients that make the energy stationary.

3.2 Worked global example: an axially loaded bar

Consider a uniform bar fixed at $x = 0$, with constant E and A, distributed load $q(x) = cx$, and no end force. Its total potential energy is

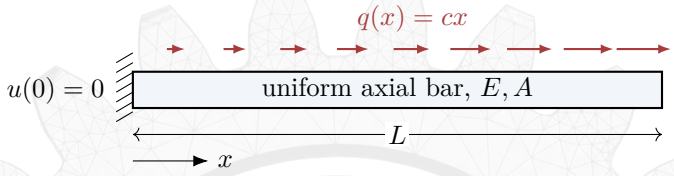


Figure 7: Axial bar used in the global Rayleigh–Ritz example. The distributed load $q(x) = cx$ increases linearly from left to right.

$$\Pi[u] = \frac{1}{2}\int_0^L EA(u')^2\,\mathrm{d}x - \int_0^L cx\,u\,\mathrm{d}x. \tag{3.5}$$

The admissible polynomial family

$$u^h = A_1x + A_2x^2 + A_3x^3 + \cdots \tag{3.6}$$

automatically satisfies $u(0) = 0$.

For one term, $u_1 = A_1x$. Substitution gives

$$\Pi(A_1) = \frac{1}{2}EAA_1^2L - \frac{cA_1L^3}{3}, \tag{3.7}$$

so

$$A_1 = \frac{cL^2}{3EA}, \qquad u_1 = \frac{cL^2x}{3EA}, \qquad \sigma_1 = \frac{cL^2}{3A}. \tag{3.8}$$

For two terms, $u_2 = A_1x + A_2x^2$. The stationarity equations are

$$EA(A_1L + A_2L^2) = \frac{cL^3}{3}, \tag{3.9}$$

$$EA\left(A_1L^2 + \frac{4}{3}A_2L^3\right) = \frac{cL^4}{4}. \tag{3.10}$$

They give

$$A_1 = \frac{7cL^2}{12EA}, \qquad A_2 = -\frac{cL}{4EA}, \tag{3.11}$$

and

$$u_2(x) = \frac{cL}{12EA}(7Lx - 3x^2), \qquad \sigma_2(x) = \frac{cL}{12A}(7L - 6x). \tag{3.12}$$

For the three-term family, the coefficients are

$$A_1 = \frac{cL^2}{2EA}, \qquad A_2 = 0, \qquad A_3 = -\frac{c}{6EA}, \tag{3.13}$$

so

$$u_3(x) = \frac{c}{6EA}(3L^2x - x^3), \qquad \sigma_3(x) = \frac{c}{2A}(L^2 - x^2). \tag{3.14}$$

This is the exact solution. Adding a fourth polynomial term returns $A_4 = 0$ and leaves the field unchanged.

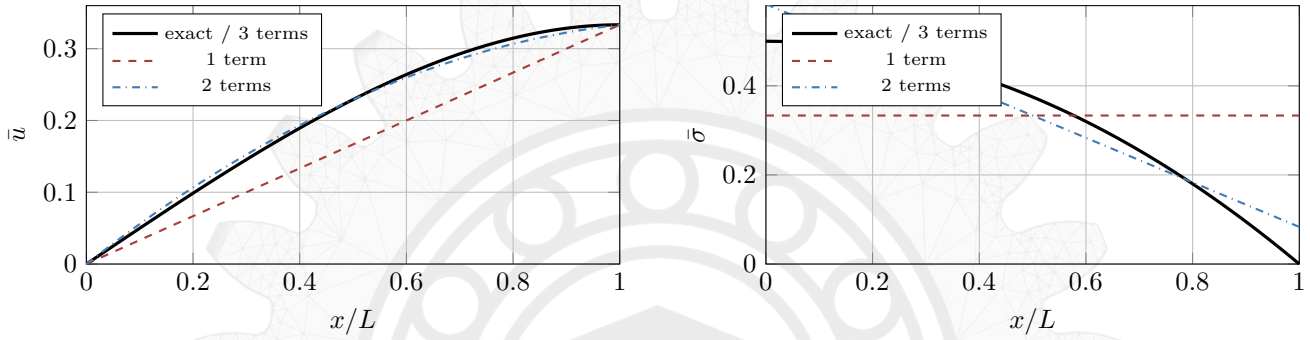
Exact reproduction by the Rayleigh–Ritz method

If the exact solution lies within the admissible family of trial functions, the Rayleigh–Ritz method reproduces it exactly. Any additional trial-function terms that are unnecessary for representing the exact solution receive zero coefficients.

To compare the approximations independently of units, define

$$r = \frac{x}{L}, \qquad \bar{u} = \frac{EA}{cL^3}u, \qquad \bar{\sigma} = \frac{A}{cL^2}\sigma. \tag{3.15}$$

The exact fields are $\bar{u} = (3r - r^3)/6$ and $\bar{\sigma} = (1 - r^2)/2$. Figure 8 shows why derivative-based quantities converge more slowly.



(a) Displacement. **(b)** Stress.

Figure 8: Global Rayleigh–Ritz convergence for the axially loaded bar.

Table 1: Relative L^2 errors for the global approximations.

Approximation	displacement error	stress error
1 term	19.80%	40.82%
2 terms	2.48%	10.21%
3 terms	0	0
4 terms	0	0

The bar example also exposes a central practical issue. Displacement error falls rapidly as the admissible family is enriched, but stress depends on u' and therefore converges more slowly.

A practical convergence observation

Stress generally converges more slowly than displacement because stress is calculated from derivatives of the displacement field. This is an extremely important characteristic of finite element simulations. A displacement solution that appears sufficiently accurate does not necessarily mean that the calculated stresses are equally accurate. If stress accuracy is important, additional mesh refinement may be required.
Refining an FE mesh is conceptually analogous to adding admissible functions to a Rayleigh–Ritz approximation: both enrich the approximation space. They are not mathematically identical procedures, because FE refinement adds local piecewise functions whereas a classical Rayleigh–Ritz method often adds global functions.

3.3 Cantilever beam: one term and two terms

Consider a cantilever of constant EI under a downward tip load P:

$$\Pi[w] = \frac{1}{2}\int_0^L EI(w'')^2\,\mathrm{d}x - Pw(L), \qquad w(0) = w'(0) = 0. \tag{3.16}$$

The one-term choice $w_1 = A_1 x^2$ gives

$$\Pi(A_1) = 2EIA_1^2 L - PA_1 L^2, \qquad A_1 = \frac{PL}{4EI}. \tag{3.17}$$

Thus

$$w_1(L) = \frac{PL^3}{4EI}, \tag{3.18}$$

which is 75% of the exact tip deflection $PL^3/(3EI)$.

Now use two admissible functions:

$$w_2(x) = A_1 x^2 + A_2 x^3. \tag{3.19}$$

Since $w_2'' = 2A_1 + 6A_2 x$,

$$\Pi(A_1, A_2) = 2EIA_1^2 L + 6EIA_1 A_2 L^2 + 6EIA_2^2 L^3 - P(A_1 L^2 + A_2 L^3). \tag{3.20}$$

The two independent stationary conditions are

$$4EIA_1 L + 6EIA_2 L^2 - PL^2 = 0, \tag{3.21}$$

$$6EIA_1 L^2 + 12EIA_2 L^3 - PL^3 = 0. \tag{3.22}$$

Solving,

$$A_1 = \frac{PL}{2EI}, \qquad A_2 = -\frac{P}{6EI}. \tag{3.23}$$

Therefore

$$\boxed{w_2(x) = \frac{Px^2}{6EI}(3L - x)}, \qquad \boxed{w_2(L) = \frac{PL^3}{3EI}}. \tag{3.24}$$

The two-term result is exact because the exact Euler–Bernoulli solution is cubic and the admissible basis $\{x^2, x^3\}$ contains every required term. No calculation with more than two functions is needed; any further independent admissible polynomial terms would receive zero coefficients.

Table 2: Cantilever tip-deflection comparison.

Approximation	$w(L)$	fraction of exact
one term, $A_1 x^2$	$PL^3/(4EI)$	0.75
two terms, $A_1 x^2 + A_2 x^3$	$PL^3/(3EI)$	1.00
exact Euler–Bernoulli solution	$PL^3/(3EI)$	1.00

3.4 Worked example: a two-dimensional two-bar truss

The same energy procedure applies directly to a structure with more than one displacement component. Consider the two-bar truss in Fig. 9. Nodes 1 and 2 are fixed, while Node 3 can move horizontally by u and vertically by v. A horizontal force P acts at Node 3. Both members have elastic modulus E and area A.

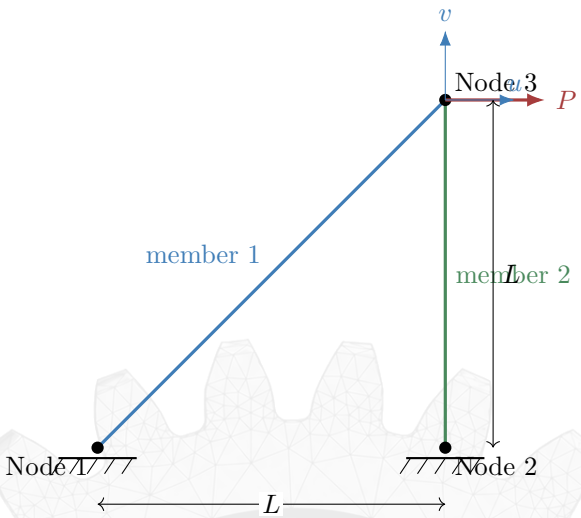


Figure 9: Two-dimensional two-bar truss. Nodes 1 and 2 are fixed; Node 3 has the two unknown displacement components u and v.

Let $\boldsymbol{q} = [u\ v]^{\mathsf{T}}$. The diagonal member has length $\sqrt{2}L$ and direction cosines $c_1 = s_1 = 1/\sqrt{2}$; the vertical member has length L, $c_2 = 0$, and $s_2 = 1$. Their small axial extensions are

$$\Delta_1 = \frac{u+v}{\sqrt{2}}, \qquad \Delta_2 = v. \tag{3.25}$$

Therefore,

$$\Pi(u,v) = \frac{EA}{4\sqrt{2}L}(u+v)^2 + \frac{EA}{2L}v^2 - Pu. \tag{3.26}$$

The two stationary equations produce

$$\frac{EA}{L}\begin{bmatrix} 1/(2\sqrt{2}) & 1/(2\sqrt{2}) \\ 1/(2\sqrt{2}) & 1+1/(2\sqrt{2}) \end{bmatrix}\begin{bmatrix} u \\ v \end{bmatrix} = \begin{bmatrix} P \\ 0 \end{bmatrix}. \tag{3.27}$$

Solving,

$$v = -\frac{PL}{EA}, \qquad u = (1+2\sqrt{2})\frac{PL}{EA}. \tag{3.28}$$

The member forces are $N_1 = \sqrt{2}P$ in tension and $N_2 = -P$ in compression. Joint equilibrium and compatibility give the same answer; because the nodal description is already finite-dimensional, the energy route is exact.

3.5 Worked example: a simply supported beam under a center load

Consider the simply supported Euler–Bernoulli beam in Fig. 10, with constant flexural rigidity EI and a concentrated load P at midspan [1].

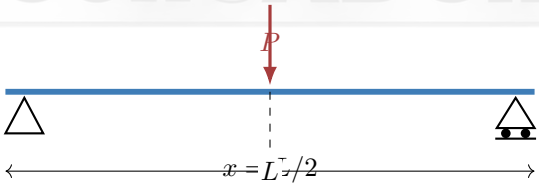


Figure 10: Simply supported Euler–Bernoulli beam with a concentrated load P at midspan.

Choose the admissible sine family

$$w_N(x) = \sum_{m=1}^{N} A_m \sin\left(\frac{(2m-1)\pi x}{L}\right). \tag{3.29}$$

Every term satisfies $w(0) = w(L) = 0$ and possesses the derivatives required by the bending energy. The potential energy is

$$\Pi[w] = \frac{1}{2}\int_0^L EI(w'')^2\,\mathrm{d}x - Pw(L/2). \tag{3.30}$$

Orthogonality of the sine functions gives, for odd $i = 1, 3, 5, \ldots$,

$$A_i = \frac{2PL^3}{EI\pi^4 i^4}\sin\left(\frac{i\pi}{2}\right). \tag{3.31}$$

Consequently,

$$w_N(L/2) = \frac{2PL^3}{EI\pi^4}\sum_{i=1,3,\ldots}^{2N-1}\frac{1}{i^4}, \tag{3.32}$$

while the exact result is $PL^3/(48EI)$. The associated moment at midspan is

$$M_N(L/2) = \frac{2PL}{\pi^2}\sum_{i=1,3,\ldots}^{2N-1}\frac{1}{i^2}, \tag{3.33}$$

compared with $PL/4$. The displacement converges much faster because moment requires two derivatives of w.

Table 3: Rayleigh–Ritz method convergence for the simply supported beam.

Number of sine terms	midspan deflection / exact	midspan moment / exact
1	98.5534%	81.0569%
2	99.7701%	90.0633%
3	99.9278%	93.3056%
4	99.9689%	94.9598%

4 From Global Rayleigh–Ritz to the Finite Element Method

Global trial functions extend across the entire structure. They can be highly efficient for simple geometry, but become cumbersome when geometry, materials, supports, or loads are complicated. The finite element method retains the same approximation and energy ideas while making the trial functions local.

4.1 Trial functions, coefficients, and nodal degrees of freedom

In a global Rayleigh–Ritz approximation,

$$u^h(x) = \sum_{i=1}^{n} A_i\phi_i(x) = \boldsymbol{\Phi}(x)\boldsymbol{A}. \tag{4.1}$$

The ϕ_i are trial or basis functions. The A_i are Ritz coefficients, generalized coordinates, or function amplitudes: each controls how much its trial function contributes. They should be called modal coordinates only if the basis functions are actual vibration modes.

In a conventional finite element,

$$\boxed{\boldsymbol{u}^h = \boldsymbol{N}\boldsymbol{d}}, \tag{4.2}$$

where $\boldsymbol{N}$ contains the local trial functions—the familiar shape functions—and $\boldsymbol{d}$ contains nodal degrees of freedom. Standard nodal shape functions satisfy

$$N_i(x_j) = \delta_{ij}. \tag{4.3}$$

Therefore

$$u^h(x_j) = \sum_i N_i(x_j)d_i = d_j, \tag{4.4}$$

so each coefficient is directly the associated nodal displacement or rotation.

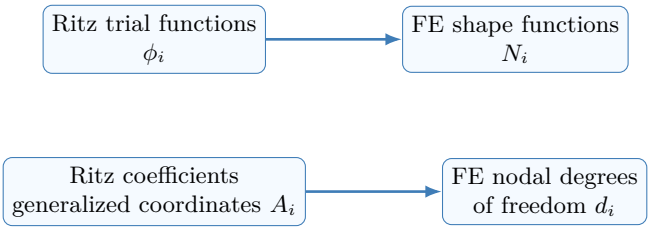


Figure 11: Conceptual transition from global Rayleigh–Ritz notation to local finite element notation.

Finite elements commonly use simple first- or second-order local polynomials because each element covers only a small region. Small size alone is not sufficient. The local approximations must connect compatibly, satisfy interpolation requirements, and form an approximation space that can be enriched by mesh refinement or higher-order interpolation. Many connected local functions can then represent a complicated global field.

4.2 From displacement interpolation to the algebraic equilibrium equations

The derivation begins with the approximate displacement field, not with the strain. Write

$$\boxed{\boldsymbol{u}^h = \boldsymbol{N}\boldsymbol{a}}, \tag{4.5}$$

where $\boldsymbol{N}$ contains the selected trial or shape functions and the bold lowercase vector $\boldsymbol{a}$ contains their unknown displacement coefficients. For a conventional finite element, these coefficients are the nodal degrees of freedom.

Strain is obtained by applying the differential operator $\boldsymbol{L}$ to the displacement field:

$$\boldsymbol{\varepsilon} = \boldsymbol{L}\boldsymbol{u}^h = \boldsymbol{L}\boldsymbol{N}\boldsymbol{a}. \tag{4.6}$$

Define

$$\boxed{\boldsymbol{B} = \boldsymbol{L}\boldsymbol{N}}, \tag{4.7}$$

so the strain-displacement relation becomes

$$\boxed{\boldsymbol{\varepsilon} = \boldsymbol{B}\boldsymbol{a}}. \tag{4.8}$$

For example, in a three-dimensional solid,

$$\boldsymbol{u}^h = \begin{bmatrix} u & v & w \end{bmatrix}^{\mathsf{T}} = \boldsymbol{N}\boldsymbol{a}, \tag{4.9}$$

with

$$\boldsymbol{N} = \begin{bmatrix} N_1 & 0 & 0 & N_2 & 0 & 0 & \cdots & N_n & 0 & 0 \\ 0 & N_1 & 0 & 0 & N_2 & 0 & \cdots & 0 & N_n & 0 \\ 0 & 0 & N_1 & 0 & 0 & N_2 & \cdots & 0 & 0 & N_n \end{bmatrix}, \tag{4.10}$$

and

$$\boldsymbol{a} = \begin{bmatrix} u_1 & v_1 & w_1 & u_2 & v_2 & w_2 & \cdots & u_n & v_n & w_n \end{bmatrix}^{\mathsf{T}}. \tag{4.11}$$

Using the engineering-strain vector,

$$\boldsymbol{\varepsilon} = \begin{bmatrix} \varepsilon_x & \varepsilon_y & \varepsilon_z & \gamma_{xy} & \gamma_{yz} & \gamma_{xz} \end{bmatrix}^{\mathsf{T}}, \tag{4.12}$$

the three-dimensional differential operator is

$$\boldsymbol{L} = \begin{bmatrix} \partial_x & 0 & 0 \\ 0 & \partial_y & 0 \\ 0 & 0 & \partial_z \\ \partial_y & \partial_x & 0 \\ 0 & \partial_z & \partial_y \\ \partial_z & 0 & \partial_x \end{bmatrix}. \tag{4.13}$$

Consequently, the block of $\boldsymbol{B} = \boldsymbol{L}\boldsymbol{N}$ associated with node i is

$$\boldsymbol{B}_i = \begin{bmatrix} N_{i,x} & 0 & 0 \\ 0 & N_{i,y} & 0 \\ 0 & 0 & N_{i,z} \\ N_{i,y} & N_{i,x} & 0 \\ 0 & N_{i,z} & N_{i,y} \\ N_{i,z} & 0 & N_{i,x} \end{bmatrix}, \qquad \boldsymbol{B} = \begin{bmatrix} \boldsymbol{B}_1 & \boldsymbol{B}_2 & \cdots & \boldsymbol{B}_n \end{bmatrix}. \tag{4.14}$$

For linear elasticity,

$$\boldsymbol{\sigma} = \boldsymbol{D}\boldsymbol{\varepsilon} = \boldsymbol{D}\boldsymbol{B}\boldsymbol{a}. \tag{4.15}$$

The total elastic strain energy is

$$U_{\text{el}} = \frac{1}{2}\int_V \boldsymbol{\varepsilon}^{\mathsf{T}}\boldsymbol{D}\boldsymbol{\varepsilon}\,\mathrm{d}V. \tag{4.16}$$

Substitution gives

$$U_{\text{el}} = \frac{1}{2}\int_V (\boldsymbol{B}\boldsymbol{a})^{\mathsf{T}}\boldsymbol{D}(\boldsymbol{B}\boldsymbol{a})\,\mathrm{d}V \tag{4.17}$$

$$= \frac{1}{2}\int_V \boldsymbol{a}^{\mathsf{T}}\boldsymbol{B}^{\mathsf{T}}\boldsymbol{D}\boldsymbol{B}\boldsymbol{a}\,\mathrm{d}V \tag{4.18}$$

$$= \boxed{\frac{1}{2}\boldsymbol{a}^{\mathsf{T}}\left[\int_V \boldsymbol{B}^{\mathsf{T}}\boldsymbol{D}\boldsymbol{B}\,\mathrm{d}V\right]\boldsymbol{a}}. \tag{4.19}$$

The row vector $\boldsymbol{a}^{\mathsf{T}}$ is not introduced arbitrarily. It appears from the transpose rule

$$(\boldsymbol{B}\boldsymbol{a})^{\mathsf{T}} = \boldsymbol{a}^{\mathsf{T}}\boldsymbol{B}^{\mathsf{T}}. \tag{4.20}$$

Because $\boldsymbol{a}$ contains coefficients rather than spatial variables, it can be moved outside the integral. Comparison with $U_{\text{el}} = \frac{1}{2}\boldsymbol{a}^{\mathsf{T}}\boldsymbol{K}\boldsymbol{a}$ identifies

$$\boxed{\boldsymbol{K} = \int_V \boldsymbol{B}^{\mathsf{T}}\boldsymbol{D}\boldsymbol{B}\,\mathrm{d}V}. \tag{4.21}$$

The stiffness integral is only one part of the finite element equations. The external loads must also be converted into nodal-force vectors that perform the same work through the interpolated displacement field. Consider body force $\boldsymbol{b}$ per unit volume, prescribed traction $\bar{\boldsymbol{t}}$ on the loaded surface S_t, and concentrated forces $\boldsymbol{P}_j$ applied at points $\boldsymbol{x}_j$. Their work is

$$W_{\text{ext}} = \int_V (\boldsymbol{u}^h)^{\mathsf{T}}\boldsymbol{b}\,\mathrm{d}V + \int_{S_t} (\boldsymbol{u}^h)^{\mathsf{T}}\bar{\boldsymbol{t}}\,\mathrm{d}S + \sum_j \boldsymbol{u}^h(\boldsymbol{x}_j)^{\mathsf{T}}\boldsymbol{P}_j. \tag{4.22}$$

Substituting $\boldsymbol{u}^h = \boldsymbol{N}\boldsymbol{a}$ gives

$$W_{\text{ext}} = \boldsymbol{a}^{\mathsf{T}}\left[\int_V \boldsymbol{N}^{\mathsf{T}}\boldsymbol{b}\,\mathrm{d}V + \int_{S_t} \boldsymbol{N}^{\mathsf{T}}\bar{\boldsymbol{t}}\,\mathrm{d}S + \sum_j \boldsymbol{N}(\boldsymbol{x}_j)^{\mathsf{T}}\boldsymbol{P}_j\right] \tag{4.23}$$

$$= \boldsymbol{a}^{\mathsf{T}}\left(\boldsymbol{F}_b + \boldsymbol{F}_t + \boldsymbol{F}_P\right) = \boldsymbol{a}^{\mathsf{T}}\boldsymbol{F}. \tag{4.24}$$

Thus, the three mechanical contributions to the consistent finite element load vector are

$$\boxed{\boldsymbol{F} = \underbrace{\int_V \boldsymbol{N}^{\mathsf{T}}\boldsymbol{b}\,\mathrm{d}V}_{\text{body-force load } \boldsymbol{F}_b} + \underbrace{\int_{S_t} \boldsymbol{N}^{\mathsf{T}}\bar{\boldsymbol{t}}\,\mathrm{d}S}_{\text{surface-traction load } \boldsymbol{F}_t} + \underbrace{\sum_j \boldsymbol{N}(\boldsymbol{x}_j)^{\mathsf{T}}\boldsymbol{P}_j}_{\text{concentrated load } \boldsymbol{F}_P}}. \tag{4.25}$$

For an individual element, the same expression is evaluated over V_e and its loaded boundary S_t^e, producing $\boldsymbol{F}_e$. A force applied directly at an element node enters the corresponding nodal-force component because $N_i(\boldsymbol{x}_j) = \delta_{ij}$. A concentrated force applied inside an element is distributed consistently to its nodes through $\boldsymbol{N}(\boldsymbol{x}_j)^{\mathsf{T}}\boldsymbol{P}_j$. A global

force applied at a shared mesh node is assembled only once; it must not be duplicated for every adjoining element. These work-equivalent load formulas are the finite element form of the general continuum expression in Eq. (2.19) [1].

The element potential energy can now be written in its complete mechanical form:

$$\boxed{\Pi_e(\boldsymbol{a}_e) = \frac{1}{2}\boldsymbol{a}_e^{\mathsf{T}}\boldsymbol{K}_e\boldsymbol{a}_e - \boldsymbol{a}_e^{\mathsf{T}}\boldsymbol{F}_e, \qquad \boldsymbol{K}_e = \int_{V_e} \boldsymbol{B}^{\mathsf{T}}\boldsymbol{D}\boldsymbol{B}\ \mathrm{d}V.} \tag{4.26}$$

After assembly over all elements, the structural potential energy is

$$\Pi(\boldsymbol{a}) = \frac{1}{2}\boldsymbol{a}^{\mathsf{T}}\boldsymbol{K}\boldsymbol{a} - \boldsymbol{a}^{\mathsf{T}}\boldsymbol{F}. \tag{4.27}$$

Matrix differentiation gives

$$\frac{\partial}{\partial \boldsymbol{a}}\left(\frac{1}{2}\boldsymbol{a}^{\mathsf{T}}\boldsymbol{K}\boldsymbol{a}\right) = \frac{1}{2}(\boldsymbol{K} + \boldsymbol{K}^{\mathsf{T}})\boldsymbol{a}. \tag{4.28}$$

For elastic stiffness, $\boldsymbol{K}^{\mathsf{T}} = \boldsymbol{K}$, so the two equal contributions cancel the prefactor $\frac{1}{2}$. Also,

$$\frac{\partial}{\partial \boldsymbol{a}}(-\boldsymbol{a}^{\mathsf{T}}\boldsymbol{F}) = -\boldsymbol{F}. \tag{4.29}$$

Therefore

$$\frac{\partial \Pi}{\partial \boldsymbol{a}} = \boldsymbol{K}\boldsymbol{a} - \boldsymbol{F} = \boldsymbol{0} \qquad \Longrightarrow \qquad \boxed{\boldsymbol{K}\boldsymbol{a} = \boldsymbol{F}}. \tag{4.30}$$

What each matrix does

- $\boldsymbol{N}$ interpolates the displacement field from nodal values.
- $\boldsymbol{L}$ contains the spatial derivatives that convert displacement components into strain components.
- $\boldsymbol{B} = \boldsymbol{L}\boldsymbol{N}$ converts nodal displacements into strains.
- $\boldsymbol{D}$ converts strains into stresses.
- $\boldsymbol{B}^{\mathsf{T}}$ converts the stress-related quantities into nodal-force contributions through energy conjugacy.
- The volume integral accumulates stiffness contributions throughout the body or element.

4.3 Worked specialization: an Euler–Bernoulli beam element

The general solid-element derivation becomes especially clear when it is specialized to a familiar beam. Consider the Euler–Bernoulli beam element in Fig. 12. Its nodal degrees of freedom are the transverse displacement and cross-section rotation at each node,

$$\boldsymbol{a}_e = \begin{bmatrix} w_i & \theta_i & w_j & \theta_j \end{bmatrix}^{\mathsf{T}}. \tag{4.31}$$

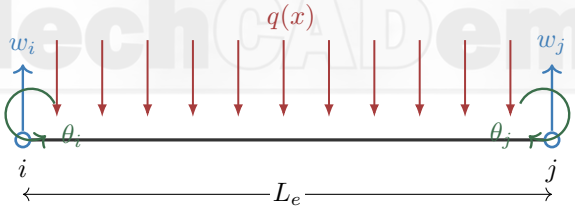


Figure 12: Euler–Bernoulli beam element with transverse displacement and rotation degrees of freedom.

Interpolate the transverse displacement as

$$w^h(x) = \boldsymbol{N}_w(x)\boldsymbol{a}_e. \tag{4.32}$$

Because $\theta = w'$, the interpolated rotation is

$$\theta^h = \frac{\mathrm{d}\boldsymbol{N}_w}{\mathrm{d}x}\boldsymbol{a}_e. \tag{4.33}$$

The bending strain measure is the curvature,

$$\kappa^h = \frac{\mathrm{d}^2 w^h}{\mathrm{d}x^2} = \underbrace{\frac{\mathrm{d}^2 \boldsymbol{N}_w}{\mathrm{d}x^2}}_{\boldsymbol{B}_b} \boldsymbol{a}_e = \boldsymbol{B}_b \boldsymbol{a}_e. \tag{4.34}$$

Thus, the beam matrix $\boldsymbol{B}_b$ contains second derivatives of the displacement shape functions. The element strain energy is

$$U_e = \frac{1}{2}\int_{L_e} EI(\kappa^h)^2 \, \mathrm{d}x \tag{4.35}$$

$$= \frac{1}{2}\boldsymbol{a}_e^{\mathsf{T}} \left[\int_{L_e} \boldsymbol{B}_b^{\mathsf{T}} EI \boldsymbol{B}_b \, \mathrm{d}x\right] \boldsymbol{a}_e. \tag{4.36}$$

Comparison with $U_e = \frac{1}{2}\boldsymbol{a}_e^{\mathsf{T}} \boldsymbol{K}_e \boldsymbol{a}_e$ identifies

$$\boxed{\boldsymbol{K}_e = \int_{L_e} \boldsymbol{B}_b^{\mathsf{T}} EI \boldsymbol{B}_b \, \mathrm{d}x.} \tag{4.37}$$

The distributed load performs the work

$$W_{q,e} = \int_{L_e} w^h q \, \mathrm{d}x = \boldsymbol{a}_e^{\mathsf{T}} \int_{L_e} \boldsymbol{N}_w^{\mathsf{T}} q \, \mathrm{d}x, \tag{4.38}$$

so its work-equivalent, or consistent, nodal-load vector is

$$\boxed{\boldsymbol{F}_{q,e} = \int_{L_e} \boldsymbol{N}_w^{\mathsf{T}} q \, \mathrm{d}x.} \tag{4.39}$$

A concentrated transverse force P_k at x_k contributes $\boldsymbol{N}_w(x_k)^{\mathsf{T}} P_k$, while a concentrated moment M_k contributes

$$\left(\frac{\mathrm{d}\boldsymbol{N}_w}{\mathrm{d}x}\right)^{\mathsf{T}}\Bigg|_{x=x_k} M_k. \tag{4.40}$$

Consequently,

$$\Pi_e = \frac{1}{2}\boldsymbol{a}_e^{\mathsf{T}} \boldsymbol{K}_e \boldsymbol{a}_e - \boldsymbol{a}_e^{\mathsf{T}} \boldsymbol{F}_e, \tag{4.41}$$

and assembly followed by stationarity again gives

$$\boxed{\boldsymbol{K}\boldsymbol{a} = \boldsymbol{F}.} \tag{4.42}$$

Why this is a useful specialization

For a solid element, $\boldsymbol{B}$ contains first derivatives of displacement shape functions because strain depends on displacement gradients. For an Euler–Bernoulli beam, curvature depends on w'', so $\boldsymbol{B}_b$ contains second derivatives. This is why a conventional beam element interpolates both w and $\theta = w'$ and must connect adjacent elements with continuous displacement and slope. The example also shows that the consistent load vector follows from the same interpolation used for displacement; it is not an arbitrary division of the applied load among the nodes.

4.4 A two-node axial bar element

For $0 \le x \le L_e$,

$$u^h = N_1 d_1 + N_2 d_2, \qquad N_1 = 1 - \frac{x}{L_e}, \quad N_2 = \frac{x}{L_e}. \tag{4.43}$$

In matrix notation,

$$u^h = \boldsymbol{N}\boldsymbol{d}, \qquad \boldsymbol{N} = \begin{bmatrix} N_1 & N_2 \end{bmatrix}, \qquad \boldsymbol{d} = \begin{bmatrix} d_1 & d_2 \end{bmatrix}^{\mathsf{T}}. \tag{4.44}$$

Differentiation gives

$$\varepsilon = \frac{\mathrm{d}u^h}{\mathrm{d}x} = \underbrace{\begin{bmatrix} -1/L_e & 1/L_e \end{bmatrix}}_{\boldsymbol{B}} \boldsymbol{d}. \tag{4.45}$$

Hence

$$\boxed{\boldsymbol{K}_e = \int_0^{L_e} \boldsymbol{B}^{\mathsf{T}} E A \boldsymbol{B}\, \mathrm{d}x = \frac{EA}{L_e}\begin{bmatrix} 1 & -1 \\ -1 & 1 \end{bmatrix}.} \tag{4.46}$$

A distributed axial load $q(x)$ produces the consistent element load

$$\boldsymbol{F}_q^{(e)} = \int_0^{L_e} \boldsymbol{N}^{\mathsf{T}} q(x)\, \mathrm{d}x. \tag{4.47}$$

4.5 Finite-element example: the same linearly loaded bar

Discretize the earlier bar into two equal linear elements of length $h = L/2$. Each element has

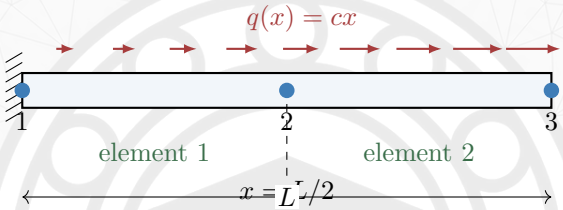


Figure 13: Two-element finite element discretization of the axially loaded bar with $q(x) = cx$.

$$\boldsymbol{K}_e = \frac{2EA}{L}\begin{bmatrix} 1 & -1 \\ -1 & 1 \end{bmatrix}. \tag{4.48}$$

Integrating $\boldsymbol{N}^{\mathsf{T}} cx$ over the two element intervals gives

$$\boldsymbol{F}^{(1)} = \frac{cL^2}{24}\begin{bmatrix} 1 \\ 2 \end{bmatrix}, \qquad \boldsymbol{F}^{(2)} = \frac{cL^2}{24}\begin{bmatrix} 4 \\ 5 \end{bmatrix}. \tag{4.49}$$

Assembly produces

$$\boldsymbol{K} = \frac{2EA}{L}\begin{bmatrix} 1 & -1 & 0 \\ -1 & 2 & -1 \\ 0 & -1 & 1 \end{bmatrix}, \qquad \boldsymbol{F} = \frac{cL^2}{24}\begin{bmatrix} 1 \\ 6 \\ 5 \end{bmatrix}. \tag{4.50}$$

With $d_1 = 0$,

$$d_2 = \frac{11cL^3}{48EA}, \qquad d_3 = \frac{cL^3}{3EA}. \tag{4.51}$$

The displacement is piecewise linear and stress is piecewise constant. Refinement makes both fields converge, but stress converges more slowly because it is derived from the displacement slope.

Table 4: Relative L^2 errors for uniform meshes of linear bar elements.

Linear FE mesh	displacement error	stress error
2 elements	5.50%	22.24%
3 elements	2.49%	15.04%
4 elements	1.41%	11.34%

For this smooth problem, the nodal displacement values on a uniform mesh happen to coincide with the exact values, but interpolation between nodes remains linear and element stress remains constant. The error table therefore measures the entire fields, not just nodal agreement.

4.6 Extension beyond structures: acoustic modes of a rigid cavity

The Rayleigh–Ritz finite-element framework is not limited to structural displacement problems. As a compact example, consider the pressure amplitude $p(x, y, z)$ in a gas- or fluid-filled cavity with rigid walls. The governing functional can be written as [1]

$$\Pi[p] = \int_V \left[p_{,x}^2 + p_{,y}^2 + p_{,z}^2 - \frac{\omega^2}{c^2} p^2 \right] \mathrm{d}V, \tag{4.52}$$

where ω is the circular frequency and c is the speed of sound. The unknown is now pressure rather than displacement, but the finite-element steps are the same.

Interpolate the pressure within element e from its nodal pressure amplitudes:

$$p^h = \boldsymbol{N}_p \boldsymbol{p}_e. \tag{4.53}$$

Its spatial gradient is

$$\nabla p^h = \begin{bmatrix} p_{,x} & p_{,y} & p_{,z} \end{bmatrix}^{\mathsf{T}} = \underbrace{\begin{bmatrix} \boldsymbol{N}_{p,x} \\ \boldsymbol{N}_{p,y} \\ \boldsymbol{N}_{p,z} \end{bmatrix}}_{\boldsymbol{B}_p} \boldsymbol{p}_e = \boldsymbol{B}_p \boldsymbol{p}_e. \tag{4.54}$$

Substitution into the element functional gives

$$\Pi_e = \boldsymbol{p}_e^{\mathsf{T}} \left[\int_{V_e} \boldsymbol{B}_p^{\mathsf{T}} \boldsymbol{B}_p \, \mathrm{d}V \right] \boldsymbol{p}_e \tag{4.55}$$

$$- \frac{\omega^2}{c^2} \boldsymbol{p}_e^{\mathsf{T}} \left[\int_{V_e} \boldsymbol{N}_p^{\mathsf{T}} \boldsymbol{N}_p \, \mathrm{d}V \right] \boldsymbol{p}_e. \tag{4.56}$$

Define the element acoustic matrices

$$\boxed{\boldsymbol{K}_{p,e} = \int_{V_e} \boldsymbol{B}_p^{\mathsf{T}} \boldsymbol{B}_p \, \mathrm{d}V, \qquad \boldsymbol{M}_{p,e} = \int_{V_e} \boldsymbol{N}_p^{\mathsf{T}} \boldsymbol{N}_p \, \mathrm{d}V.} \tag{4.57}$$

The factor of two produced by differentiating each quadratic form cancels from the stationary equation. After assembly, stationarity with respect to the global nodal-pressure vector $\boldsymbol{p}$ gives

$$\boxed{\left(\boldsymbol{K}_p - \frac{\omega^2}{c^2} \boldsymbol{M}_p \right) \boldsymbol{p} = \boldsymbol{0}.} \tag{4.58}$$

This is a generalized eigenvalue problem,

$$\boldsymbol{K}_p \boldsymbol{p} = \lambda \boldsymbol{M}_p \boldsymbol{p}, \qquad \lambda = \frac{\omega^2}{c^2}. \tag{4.59}$$

For each computed eigenvalue λ_r,

$$\boxed{\omega_r = c\sqrt{\lambda_r}, \qquad f_r = \frac{\omega_r}{2\pi}.} \tag{4.60}$$

The associated eigenvector gives the relative nodal pressure amplitudes of the acoustic mode. A rigid wall imposes zero normal particle velocity, which leads to the natural boundary condition

$$\frac{\partial p}{\partial n} = 0. \tag{4.61}$$

The constant-pressure field is therefore an admissible zero-frequency mode. The remaining eigenpairs describe the nonzero resonant pressure patterns of the cavity.

The same finite-element pattern

The structural and acoustic equations have different physical meanings but the same mathematical construction:

$$\text{interpolate the field} \longrightarrow \text{differentiate it} \longrightarrow \text{substitute into a functional}$$
$$\longrightarrow \text{make the functional stationary} \longrightarrow \text{obtain the finite-element equations.}$$

For a static structure this produces $\boldsymbol{K}\boldsymbol{a} = \boldsymbol{F}$. For a free acoustic cavity it produces the eigenvalue problem $\boldsymbol{K}_p\boldsymbol{p} = (\omega^2/c^2)\boldsymbol{M}_p\boldsymbol{p}$.

5 Thermal Strains, Initial Strains, and Residual Stresses

The mechanical-load formulation above assumes that stress is produced only by the strain associated with the unknown displacement field. A structure may, however, possess a strain that it would undergo without mechanical resistance—for example, thermal expansion, shrinkage, swelling, or an imposed lack of fit. It may also contain a known initial or residual stress before the additional mechanical loading is applied. These effects enter naturally through the same energy formulation [1].

Let $\boldsymbol{\varepsilon}^*$ denote the total prescribed stress-free initial strain,

$$\boldsymbol{\varepsilon}^* = \boldsymbol{\varepsilon}_{\text{th}} + \boldsymbol{\varepsilon}_0, \tag{5.1}$$

where $\boldsymbol{\varepsilon}_{\text{th}}$ is thermal strain and $\boldsymbol{\varepsilon}_0$ may represent another imposed initial strain. Let $\boldsymbol{\sigma}_0$ be an independently prescribed initial or residual stress. For small-strain linear elasticity, write

$$\boxed{\boldsymbol{\sigma} = \boldsymbol{D}\,(\boldsymbol{\varepsilon} - \boldsymbol{\varepsilon}^*) + \boldsymbol{\sigma}_0.} \tag{5.2}$$

The same physical source should not be specified twice. For example, if a residual stress is generated by a known eigenstrain and that eigenstrain is modeled through $\boldsymbol{\varepsilon}^*$, the corresponding stress should not also be entered independently as $\boldsymbol{\sigma}_0$.

For an isotropic three-dimensional material subjected to a temperature change ΔT,

$$\boldsymbol{\varepsilon}_{\text{th}} = \alpha \Delta T \begin{bmatrix} 1 & 1 & 1 & 0 & 0 & 0 \end{bmatrix}^{\mathsf{T}}, \tag{5.3}$$

where α is the coefficient of thermal expansion. The strain vector and constitutive matrix must be specialized consistently for a one- or two-dimensional assumption.

Apart from constants that do not depend on the unknown nodal displacement vector, the element elastic energy is

$$U_{\text{el},e} = \int_{V_e} \left[\frac{1}{2}\boldsymbol{\varepsilon}^{\mathsf{T}}\boldsymbol{D}\boldsymbol{\varepsilon} - \boldsymbol{\varepsilon}^{\mathsf{T}}\boldsymbol{D}\boldsymbol{\varepsilon}^* + \boldsymbol{\varepsilon}^{\mathsf{T}}\boldsymbol{\sigma}_0 \right] \mathrm{d}V. \tag{5.4}$$

Substituting $\boldsymbol{\varepsilon} = \boldsymbol{B}\boldsymbol{a}_e$ gives

$$U_{\text{el},e} = \frac{1}{2}\boldsymbol{a}_e^{\mathsf{T}}\boldsymbol{K}_e\boldsymbol{a}_e - \boldsymbol{a}_e^{\mathsf{T}} \underbrace{\int_{V_e} \boldsymbol{B}^{\mathsf{T}}\boldsymbol{D}\boldsymbol{\varepsilon}^* \,\mathrm{d}V}_{\boldsymbol{F}_{\varepsilon^*}^{(e)}} + \boldsymbol{a}_e^{\mathsf{T}} \underbrace{\int_{V_e} \boldsymbol{B}^{\mathsf{T}}\boldsymbol{\sigma}_0 \,\mathrm{d}V}_{\boldsymbol{F}_{\sigma_0}^{(e)}}. \tag{5.5}$$

Consequently, the element potential energy becomes

$$\Pi_e = \frac{1}{2}\boldsymbol{a}_e^{\mathsf{T}}\boldsymbol{K}_e\boldsymbol{a}_e - \boldsymbol{a}_e^{\mathsf{T}}\left(\boldsymbol{F}_{\text{ext}}^{(e)} + \boldsymbol{F}_{\varepsilon^*}^{(e)} - \boldsymbol{F}_{\sigma_0}^{(e)}\right), \tag{5.6}$$

and stationarity produces

$$\boxed{\boldsymbol{K}_e\boldsymbol{a}_e = \boldsymbol{F}_{\text{ext}}^{(e)} + \boldsymbol{F}_{\varepsilon^*}^{(e)} - \boldsymbol{F}_{\sigma_0}^{(e)}.} \tag{5.7}$$

Thus, under the present assumptions, prescribed initial strains and stresses appear as equivalent nodal loads. They do not change $\boldsymbol{K}_e$ unless the material matrix, geometry, or other stiffness-defining property also changes. After the nodal displacements are found, stress must be recovered from

$$\boxed{\boldsymbol{\sigma} = \boldsymbol{D}\,(\boldsymbol{B}\boldsymbol{a}_e - \boldsymbol{\varepsilon}^*) + \boldsymbol{\sigma}_0.} \tag{5.8}$$

Uniformly heated axial bar

For a two-node bar with constant E, A, α, and ΔT,

$$\boldsymbol{F}_{\text{th}}^{(e)} = \int_0^{L_e} \boldsymbol{B}^{\mathsf{T}} E\alpha\Delta T\, A \, \mathrm{d}x = EA\alpha\Delta T \begin{bmatrix} -1 \\ 1 \end{bmatrix}.$$

If the bar is free to expand, its nodal displacement difference is $d_2 - d_1 = \alpha\Delta T L_e$, so $\varepsilon = \varepsilon_{\text{th}}$ and the stress is zero. If both ends are restrained, the displacement strain is zero and

$$\sigma = -E\alpha\Delta T.$$

The same thermal strain therefore produces either free expansion or compressive stress depending on the kinematic constraints.

An initial residual-stress field contributes through $\boldsymbol{F}_{\sigma_0}^{(e)}$. A physically admissible residual-stress field is normally self-equilibrated over the complete body: element contributions may cancel during assembly even though nonzero local residual stress remains. This is why the stress-recovery equation must retain $\boldsymbol{\sigma}_0$ even when its assembled resultant is zero.

6 Deeper Understanding After the Method Is Clear

6.1 Why the continuum problem becomes finite

The exact field can be any admissible function, so the search is infinite-dimensional. The approximation

$$u^h = \sum_{i=1}^{n} A_i \phi_i \tag{6.1}$$

restricts the search to n chosen directions. Once the functions are fixed, ordinary multivariable calculus determines a finite number of coefficients.

6.2 Finite coefficient equations versus pointwise equilibrium

The conditions $\partial\Pi/\partial A_i = 0$ test only the selected trial directions. They enforce equilibrium within that approximation space, not automatically at every material point. If instead an arbitrary admissible perturbation $v(x)$ is introduced into the axial-bar functional by $u_t = u + tv$, differentiation at $t = 0$ gives

$$\int_0^L EAu'v' \, \mathrm{d}x - \int_0^L qv \, \mathrm{d}x - Pv(L) = 0. \tag{6.2}$$

Integration by parts yields the exact local equation and natural boundary condition:

$$\frac{\mathrm{d}}{\mathrm{d}x}(EAu') + q = 0, \qquad EAu'(L) = P. \tag{6.3}$$

The energy statement therefore contains pointwise equilibrium, but the Rayleigh–Ritz method tests it only through a finite set of admissible directions.

6.3 Why displacement usually converges faster than stress

For an axial bar, $\sigma = Eu'$. Differentiation magnifies differences between nearby approximate functions. A displacement plot may look smooth and converged while its derivative, and therefore stress, still changes materially with refinement. For beams and plates, moments or stresses can depend on second derivatives, making the effect stronger.

For example, on $0 \le x \le 1$, the functions $f_1 = 4x(1-x)$ and $f_2 = \sin(\pi x)$ are visually similar. Their first derivatives, $4 - 8x$ and $\pi\cos(\pi x)$, differ more noticeably; their second derivatives, -8 and $-\pi^2\sin(\pi x)$, differ still more.

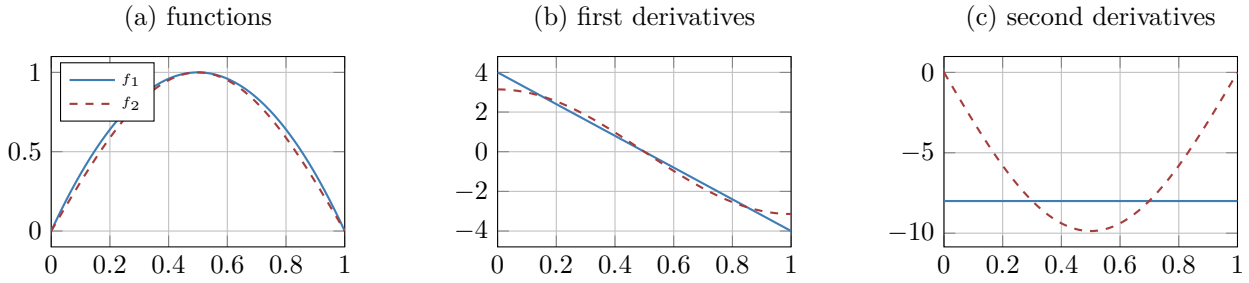


Figure 14: Differentiation magnifies differences between two initially similar functions.

What to monitor in an FE convergence study

Convergence must be judged using the quantity that drives the engineering decision. If stress, moment, strain energy, or a local reaction is important, do not accept a mesh merely because global displacement has stabilized. Examine the derivative-based quantity itself and refine locally where necessary.

6.4 Artificial stiffness: physical meaning, consequences, and remedies

Artificial stiffness is nonphysical resistance created by the approximation, not by the actual material or geometry. A displacement-based element is allowed to deform only through the patterns spanned by its shape functions. If a physically valid deformation mode is absent or unintentionally constrained, the computed element must use a more energetically expensive pattern. It then behaves as though additional stiffness had been added.

This idea is the element-level counterpart of an overly restricted Rayleigh–Ritz space. Cook et al. show that displacement assumptions generally overestimate overall stiffness and discuss the resulting bounds and stress limitations in their treatment of the Rayleigh–Ritz method (4th ed., Sec. 4.5, pp. 146–151) [1]. Their element discussions also identify parasitic shear and locking in low-order formulations (Sec. 3.6, especially pp. 95–99) and interpret locking as an implicit penalty constraint (Sec. 13.4, pp. 495–500) [1].

A physical example: a slender member in bending. In pure Euler–Bernoulli bending, cross sections rotate while transverse shear strain should vanish. A low-order displacement element may be unable to represent the bending rotation without also producing a spurious shear strain. The constitutive law assigns energy to that nonphysical shear. As the member becomes slender, the artificial shear energy can dominate the true bending energy, causing *shear locking*: the element predicts far too little deflection and behaves dramatically too stiff. Cook et al. give the corresponding bending-stiffness overestimate as scaling approximately with $(L/t)^2$ for the locking example discussed on p. 543 [1].

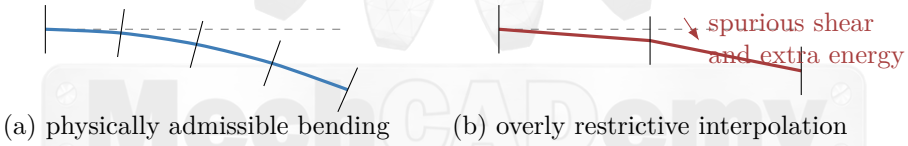


Figure 15: Artificial stiffness in bending: an inadequate interpolation can force spurious shear into a deformation that should be nearly shear-free.

The consequences can include:

- underpredicted displacements and rotations;
- incorrect stress distributions, sometimes too low in one region and too high in another;
- slow convergence under mesh refinement;
- poor performance for specific shapes, aspect ratios, thicknesses, or material limits;
- locking, including shear, membrane, or volumetric locking where the formulation imposes excessive constraints.

Artificial stiffness must be distinguished from real stiffness. Real stiffness changes when E, geometry, thickness, boundary conditions, or actual load path changes. Artificial stiffness changes when the approximation is altered even though the physical problem is unchanged.

Possible remedies depend on the source:

- refine the mesh so local functions can combine into richer deformation patterns;
- use higher-order or better-suited element formulations;
- select elements designed for the structural behavior and thickness regime;
- use mixed, assumed-strain, enhanced-strain, or incompatible-mode formulations when appropriate;
- use reduced or selective integration when it removes an excessive constraint without introducing unstable zero-energy modes;
- avoid unnecessarily restrictive kinematic assumptions and poor element distortion.

Major modeling takeaway

A finite element solution may satisfy the assembled algebraic equilibrium equations and still be inaccurate if the assumed displacement field imposes unintended kinematic constraints.
An approximation space that is too restrictive cannot represent all physically admissible deformation patterns. The resulting solution may therefore be artificially stiff.

For nested admissible spaces $V_1 \subset V_2 \subset \cdots$, enriching the space cannot raise the minimum total potential energy. Under prescribed loads, displacement-based solutions approach the exact solution from the kinematically restricted side, although individual displacement components and local stresses do not necessarily provide simple pointwise bounds [1].

7 Connection to Weighted-Residual and Galerkin Methods

The energy route is natural for conservative structural problems because an appropriate functional exists. A weighted-residual method begins instead from a governing differential equation $\mathcal{L}(u) = f$. For an approximation u^h, define the residual

$$R = \mathcal{L}(u^h) - f. \tag{7.1}$$

The method requires

$$\int_D w_i R \, \mathrm{d}D = 0. \tag{7.2}$$

Galerkin's method chooses weights from the same family used to approximate the unknown. After integration by parts, the weak form often has the same derivative order and, for suitable symmetric structural problems, produces the same FE equations as the Rayleigh–Ritz method [2, 3, 4, 5].

Table 5: Two common routes to finite element equations.

	Rayleigh–Ritz method	Weighted residual / Galerkin
Starting point	Functional such as total potential energy	Governing differential equation
Main operation	Make the functional stationary in an admissible finite space	Make the residual orthogonal to selected weights
Classical functional required?	Yes	No
Typical structural outcome	$\boldsymbol{K}\boldsymbol{a} = \boldsymbol{F}$	Often the same symmetric system

8 Problem for Further Study

Isotropic plate under lateral pressure

An isotropic thin plate with flexural rigidity D, Poisson's ratio ν, transverse displacement $w(x,y)$, and lateral pressure $q(x,y)$ has the functional [1]

$$\Pi[w] = \frac{D}{2}\iint_A \left\{ (w_{,xx}+w_{,yy})^2 - 2(1-\nu)\left[w_{,xx}w_{,yy} - w_{,xy}^2\right] - \frac{2qw}{D} \right\} \mathrm{d}A. \tag{8.1}$$

Using the finite-element approximation

$$w^h = \boldsymbol{N}_w \boldsymbol{a}_e, \tag{8.2}$$

derive the finite-element formulation. Your solution should:

1. define an appropriate plate-curvature vector;
2. derive the curvature-displacement matrix $\boldsymbol{B}_b$;
3. obtain the element bending-stiffness matrix;
4. obtain the consistent element load vector associated with $q(x,y)$; and
5. show how element assembly and stationarity produce the global equilibrium equations.

No particular plate shape functions are required. Express the result in terms of $\boldsymbol{N}_w$, its spatial derivatives, and the plate constitutive matrix.

9 Compact Formula Summary

Energy

$$\Pi = U_{\mathrm{el}} - W_{\mathrm{ext}}, \qquad U_e(\varepsilon) = \int_0^{\varepsilon} \sigma(\tilde{\varepsilon})\,\mathrm{d}\tilde{\varepsilon},$$

$$U_{e,\mathrm{linear}} = \tfrac{1}{2}\sigma\varepsilon, \qquad U_{\mathrm{el,bar}} = \tfrac{1}{2}\int_0^L EA(u')^2\,\mathrm{d}x,$$

$$U_{\mathrm{el,beam}} = \tfrac{1}{2}\int_0^L EI(w'')^2\,\mathrm{d}x, \qquad U_{\mathrm{el,solid}} = \tfrac{1}{2}\int_V \boldsymbol{\varepsilon}^{\mathsf{T}}\boldsymbol{D}\boldsymbol{\varepsilon}\,\mathrm{d}V.$$

Approximation and finite elements

$$u^h = \sum_i A_i\phi_i, \qquad \frac{\partial \Pi}{\partial A_i} = 0,$$

$$\boldsymbol{u}^h = \boldsymbol{N}\boldsymbol{a}_e, \qquad \boldsymbol{\varepsilon} = \boldsymbol{B}\boldsymbol{a}_e,$$

$$\boldsymbol{\sigma} = \boldsymbol{D}\boldsymbol{\varepsilon}, \qquad \boldsymbol{K}_e = \int_{V_e} \boldsymbol{B}^{\mathsf{T}}\boldsymbol{D}\boldsymbol{B}\,\mathrm{d}V.$$

Mechanical loads and prescribed initial fields

$$\boldsymbol{F}_e = \int_{V_e} \boldsymbol{N}^{\mathsf{T}}\boldsymbol{b}\,\mathrm{d}V + \int_{S_t^e} \boldsymbol{N}^{\mathsf{T}}\bar{\boldsymbol{t}}\,\mathrm{d}S + \sum_j \boldsymbol{N}(\boldsymbol{x}_j)^{\mathsf{T}}\boldsymbol{P}_j,$$

$$\boldsymbol{K}_e\boldsymbol{a}_e = \boldsymbol{F}_{\mathrm{ext}}^{(e)} + \boldsymbol{F}_{\varepsilon^*}^{(e)} - \boldsymbol{F}_{\sigma_0}^{(e)}, \qquad \boldsymbol{\sigma} = \boldsymbol{D}(\boldsymbol{B}\boldsymbol{a}_e - \boldsymbol{\varepsilon}^*) + \boldsymbol{\sigma}_0.$$

10 Concluding Perspective

The energy route is one continuous chain. Deformation stores strain energy; external loads perform work; stable equilibrium locally minimizes total potential energy. A continuum has infinitely many displacement degrees of freedom, so the Rayleigh–Ritz method restricts the search to a finite admissible family. The finite element method localizes that family, identifies its coefficients with nodal degrees of freedom, and assembles many simple local approximations into a global model.

The method is powerful precisely because kinematics, material behavior, loading, approximation, energy, and equilibrium meet in one system. The same fact explains its limitations: if the assumed kinematics are too restrictive, the algebraic equations can be solved perfectly while the physical solution remains artificially stiff.

Central message

$\boldsymbol{K}\boldsymbol{a} = \boldsymbol{F}$ is the end of the derivation, not the beginning. Understanding the assumptions that created $\boldsymbol{K}$ is essential for interpreting the answer.

CAD FEA Design MechCADemy

References

[1] R. D. Cook, D. S. Malkus, M. E. Plesha, and R. J. Witt, *Concepts and Applications of Finite Element Analysis*, 4th ed., John Wiley & Sons, 2002.

[2] D. L. Logan, *A First Course in the Finite Element Method*, 4th ed., Thomson, 2007.

[3] F. L. Stasa, *Applied Finite Element Analysis for Engineers*, CBS College Publishing, 1985.

[4] O. C. Zienkiewicz and R. L. Taylor, *The Finite Element Method: The Basis*, 5th ed., Butterworth–Heinemann, 2000.

[5] K.-J. Bathe, *Finite Element Procedures*, Prentice Hall, 1996.

CAD FEA Design MechCADemy